

## Critical magnetization at antiphase boundaries of magnetic binary alloys

C. Varea and A. Robledo\*

*División de Estudios de Posgrado, Facultad de Química, Universidad Nacional Autónoma de México, México 04510, Distrito Federal, Mexico*

(Received 16 March 1987)

We analyze the critical behavior of the magnetization at antiphase boundaries (APB's) of magnetic alloys. For an Ising-like model alloy in the mean-field approximation the symmetry-breaking APB's induce, within a certain range of bulk compositions, local magnetic order above the Curie temperature. This purely interfacial critical behavior explains the self-reversal thermoremanent magnetism of the ilmenite ( $\text{FeTiO}_2$ ) haematite ( $\text{Fe}_2\text{O}_3$ ) solid-solution series ( $\text{Ilm}_x\text{Hem}_{1-x}$ ).

### I. INTRODUCTION

Antiphase boundaries (APB's) are coherent interfaces that separate domains of the same ordered phase in ordering alloys.<sup>1,2</sup> They result from the symmetry breaking during ordering processes which can start in different places in a disordered lattice. The APB's form when two such regions come into contact where they introduce a local variation in composition. In this paper we show that antiphase boundaries of model magnetic ordering alloys allow naturally for the occurrence of pure interfacial criticality. This observation is relevant because experimental verification of this phenomenon may already be found among the known properties of certain materials, such as the self-reversal in the magnetization of some thermoremanent magnetic alloys.<sup>3-5</sup> This and the inverse effect, the pinning of chemical order by magnetic domain walls, are analogous to the pure surface transitions that take place in semi-infinite ferromagnets.<sup>6</sup> The latter have been recently observed experimentally in the free surfaces of Cr (Ref. 7) and Gd.<sup>8</sup>

The possibility for a surface to form a separate phase from the bulk has been discussed by many authors.<sup>6</sup> Different kinds of singularities appear in the free energy that describes the inhomogeneity, and these have been grouped in a "surface phase diagram" often described in ferromagnetic language. There, a natural field parameter is the ratio  $\Delta = J_1/J$  of the surface to bulk values of the exchange couplings between spins. In the absence of both surface and bulk magnetic fields, and provided  $\Delta$  is less than a critical value  $\Delta_c$  and  $g \equiv \Delta - \Delta_c < 0$ , the surface magnetizes when the bulk does at the critical temperature  $T_C^B$ . However, the magnetization  $m_1$  at the surface layer vanishes with an exponent different from that of the bulk. For sufficiently enhanced coupling at the surface layer,  $g > 0$ , a pure surface transition occurs at  $T_C^S > T_C^B$ , indicating the existence of surface magnetic order at temperatures at which the bulk is still disordered. At  $g = 0$  there is a "special" multicritical point where the two regimes merge.<sup>6</sup>

In the case of the surface of a simple ferromagnet, this variety of behavior results from the different possible relaxation effects near the surface that imply different values for the spin couplings. However, these relaxation

effects are not the only mechanism through which pure surface transitions can arise. For example, we have found<sup>9</sup> that the critical behavior at a model semipermeable membrane separating a binary mixture into two fluids is equivalent to that of a semi-infinite ferromagnet with surface enhancement. But here this enhancement is determined by the undersaturation and inhomogeneity imposed by the membrane, and particle-particle interactions are not altered anywhere. Grain boundaries, antiphase boundaries, and other kinds of interfaces present in multidomain solids impose also variations in density and composition and interfacial critical behavior might be expected to occur under certain conditions. Since these features reside in the interior of the material the interfacial behavior may not be directly accessible to experiment, however there may be some macroscopic consequences associated to it. The self-reversal in the magnetization of titanohaematites<sup>3-5</sup> may provide an example of such measurable critical behavior. It has been shown<sup>3-5</sup> that in these materials the mechanism that triggers self-reversal is the magnetization of the APB's at temperatures above the Curie temperature,  $T_C^B$ , and, in the language we just described, the composition profile at the APB's would provide the enhancement factor for a purely interfacial transition. If the thermal history of the material is one of progressive cooling, the magnetic domains occurring at  $T < T_C^B$  throughout the sample would be pinned by the APB's and will therefore coincide in space with the antiphase domains. In these ferromagnetic materials, antiphase domains grow ferromagnetically coupled across the APB's but they exhibit a magnetization opposed to that of the APB's.<sup>3-5</sup>

Below we analyze the magnetic behavior of model  $L2_0$  binary magnetic ordering alloys. Although these systems have a very simple crystalline structure when compared with the rhombohedral sesquioxide structure<sup>10</sup> of the titanohaematites, their rich bulk behavior and their ability to form APB's (Refs. 4 and 5) make them good candidates for studying in them the mechanism of self-reversal described above. For appropriate ratios of the chemical to magnetic interactions,  $L2_0$  magnetic alloys order chemically at a temperature higher than the Curie temperature. Under these circumstances chemical ordering either promotes or depresses the appearance of

magnetic order. In the latter case the Curie temperature of the disordered alloy,  $T_{md}$ , that corresponds to a metastable bulk state, is higher than that for the ordered alloy,  $T_{mo}$ . (Note that we use other notations for  $T_C^B$ .) The presence of an APB introduces some degree of disorder in the system, which may be large enough as to allow for the spontaneous magnetization of the APB at a temperature  $T_C^{APB} > T_{mo}$ . We have calculated the composition and magnetization profiles within the mean-field approximation in an Ising-like magnetic alloy that contains (001) APB's,<sup>11</sup> and we find pure magnetic interfacial transitions in all cases for which  $T_{md} > T_{mo}$ . We find also that the ferromagnetic (or antiferromagnetic) coupling between the two antiphase domains is strongly dependent upon the sample global composition.

## II. MODEL MAGNETIC ALLOY: BULK PROPERTIES

The model (Ising) magnetic alloy consists of two types of atoms,  $A$  and  $B$ , with magnetic moments  $S_A$  and  $S_B$ , respectively, on a body-centered-cubic lattice with only nearest-neighbor (chemical and magnetic) interactions. At each lattice site  $i$ , the probability of finding an atom  $A$  with its spin pointing up (down) is  $n_{Ai}^+$  ( $n_{Ai}^-$ ), and similarly  $n_{Bi}^+$  ( $n_{Bi}^-$ ) for atoms of kind  $B$ . The total occu-

pancy of each species is  $n_{Ai} = n_{Ai}^+ + n_{Ai}^-$  and  $n_{Bi} = n_{Bi}^+ + n_{Bi}^-$ , with the restriction  $n_{Ai} + n_{Bi} = 1$  when there are no vacancies on the lattice. Ordered bulk phases are accounted for by dividing the lattice into two equivalent and interpenetrating sublattices, 1 and 2, such that nearest-neighbor pairs belong to different sublattices. The occupancies defined above take only two values denoted by letting the subindex  $i$  be either 1 or 2. Therefore, the concentration  $x$  of atoms of kind  $A$  is  $x = (n_{A1} + n_{A2})/2$ .

The magnetizations of the species  $A$  and  $B$  are measured through the order parameters  $\xi_l = (n_{Al}^+ - n_{Al}^-)/n_{Al}$  and  $\eta_l = (n_{Bl}^+ - n_{Bl}^-)/n_{Bl}$ ,  $l = 1, 2$ , and the chemical order is described by the order parameter  $\xi_l = n_{Al} - n_{Bl}$ ,  $l = 1, 2$ . With this notation the chemical energy in mean-field approximation is given by

$$U_{\text{chem}} = -\frac{ZN}{4} [\Lambda \xi_1 \xi_2 + \nu (\xi_1 + \xi_2)] + \text{const} . \quad (1)$$

$\Lambda$  is a heat of mixing parameter,  $\Lambda = 2u_{AB} - u_{AA} - u_{BB}$ , and  $\nu = u_{BB} - u_{AA}$  is a measure of the difference in cohesive energy of the two species. The coordination number is  $Z = 8$  and the chemical interaction energies for the pairs  $AA$ ,  $AB$ , and  $BB$  are  $u_{AA}$ ,  $u_{AB}$ , and  $u_{BB}$ , respectively. Within the same approximation, the magnetic energy is written in the form

$$U_{\text{mag}} = -\frac{ZN}{4} \{ K_{AA}(1 + \xi_1)(1 + \xi_2)\xi_1\xi_2 + K_{AB}[(1 + \xi_1)(1 - \xi_2)\xi_1\eta_2 + (1 - \xi_1)(1 + \xi_2)\xi_2\eta_1] + K_{BB}(1 - \xi_1)(1 - \xi_2)\eta_1\eta_2 \} , \quad (2)$$

where the magnetic interaction parameters  $K_{\alpha\beta}$  ( $\alpha, \beta = A, B$ ) are given by  $K_{\alpha\beta} = S_\alpha S_\beta J_{\alpha\beta}$  and where  $J_{\alpha\beta}$  are the magnetic couplings. The grand potential  $\omega$ , per site or unit cell, at temperature  $k_B T$  and chemical potential difference  $\mu_A - \mu_B$ , is

$$\begin{aligned} \omega = & \frac{k_B T}{4} \left\{ \sum_{l=1,2} 2[(1 + \xi_l) \ln(1 + \xi_l) + (1 - \xi_l) \ln(1 - \xi_l)] \right. \\ & + (1 + \xi_l)[(1 + \xi_l) \ln(1 + \xi_l) + (1 - \xi_l) \ln(1 - \xi_l)] \\ & \left. + (1 - \xi_l)[(1 + \eta_l) \ln(1 + \eta_l) + (1 - \eta_l) \ln(1 - \eta_l)] \right\} \\ & + \frac{Z}{2} \{ \Lambda \xi_1 \xi_2 + [\nu - (\mu_A - \mu_B)](\xi_1 + \xi_2) + K_{AA}(1 + \xi_1)(1 + \xi_2)\xi_1\xi_2 \\ & + K_{AB}[(1 + \xi_1)(1 - \xi_2)\xi_1\eta_2 + (1 - \xi_1)(1 + \xi_2)\xi_2\eta_1] + K_{BB}(1 - \xi_1)(1 - \xi_2)\eta_1\eta_2 \} . \end{aligned} \quad (3)$$

The grand potential  $\omega$  permits different kinds of phase diagrams. When  $\Lambda < 0$  the alloy orders chemically in the sense that the sublattices have different average compositions at low temperatures. Since magnetic order is also present at low temperatures, two different classes of behavior may arise: the alloy magnetizes in the chemically disordered phase, or, otherwise it does so in the ordered phase. The alloy concentration determines which kind of behavior takes place. To see this, we consider two limiting cases, an alloy with no magnetic order

( $\xi_l = \eta_l = 0$  for all  $T$ ) and an alloy with no chemical order ( $\xi_l = 2x - 1$  for all  $T$ ). In the first case the model predicts an order-disorder transition of the second kind occurring at all compositions with an ordering transition temperature  $T_o$  given by

$$k_B T_o = -\frac{1}{2} \Lambda x (1 - x) . \quad (4)$$

In the second case, the Curie or Néel temperature of the disordered alloy  $T_{md}$  is given by one of the roots of the equation

$$(k_B T)^4 - 4(k_B T)^2 [K_{AA}^2 x^2 + 2K_{AB}^2 x(1-x) + K_{BB}^2 (1-x)^2] + 16x^2(1-x)^2 [K_{AA}K_{BB} - K_{AB}^2]^2 = 0. \quad (5)$$

In general, when  $T_0 > T_{md}$  the alloy orders and the critical temperature for the onset of spontaneous magnetization  $T_{mo}$  is influenced by the chemical order.  $T_{mo}$  is given by one of the roots of the equation

$$(k_B T)^4 - (k_B T)^2 \{ K_{AB}^2 [(1+\xi_1)(1-\xi_2) + (1-\xi_1)(1+\xi_2)] + K_{AA}^2 (1+\xi_2)(1+\xi_1) + K_{BB}^2 (1-\xi_1)(1-\xi_2) \} + (1-\xi_1^2)(1-\xi_2^2) [K_{AA}K_{BB} - K_{AB}^2]^2 = 0, \quad (6)$$

where  $\xi_1$  and  $\xi_2$  are determined by minimizing the purely chemical term of  $\omega$  with respect to the occupancies, with the composition imposed restriction  $\xi_1 + \xi_2 = 2(2x - 1)$ . This implies that

$$k_B T \ln \left[ \frac{(1+\xi_1)(1-\xi_2)}{(1-\xi_1)(1+\xi_2)} \right] - 2Z \Lambda \xi_1 \xi_2 = 0, \quad (7)$$

to which we associate an effective chemical potential  $\mu^* = \nu - \mu_A + \mu_B$  given by

$$\mu^* = k_B T \ln \left[ \frac{1+\xi_1}{1-\xi_1} \right] - 2Z \Lambda \xi_2. \quad (8)$$

The magnetic order of alloys which magnetize in the chemically ordered phase is enhanced or depressed by the degree of chemical order.

The parameter which determines the two kinds of behavior described is  $\gamma = 1 - 2|K_{AB}| / (|K_{AA}| + |K_{BB}|)$ . When  $\gamma < 0$  magnetic order is favored in the ordered alloy since the majority of the bonds in this state are  $A-B$  bonds, and then  $T_{mo} > T_{md}$ . On the other hand,  $\gamma > 0$  implies that magnetic order is assisted by segregation of species, so that in the ordered alloy one may have  $T_{mo} < T_{md}$ . In the model perfect single crystal the true transition temperature is  $T_{mo}$ , but crystal defects which diminish the number of  $AB$  bonds increase the magnetization transition eventually exposing  $T_{md}$  (and making it available to experiment in real systems). Figure 1 shows different kinds of behavior obtained from four different sets of magnetic interaction parameters. In Fig. 1(a) we show the dependence of the three transition temperatures  $T_o$ ,  $T_{mo}$ , and  $T_{md}$  on composition for an alloy in which one component is ferromagnetic, the other antiferromagnetic, and the mixed coupling constant is ferromagnetic, and since  $\gamma < 0$ ,  $T_{mo} > T_{md}$ . We also observe an enhancement of order over magnetization as the composition approaches  $x = \frac{1}{2}$ . In Fig. 1(b) we observe the behavior of the same quantities when the alloy is composed of two ferromagnetic species but there is an antiferromagnetic coupling between them. In Figs. 1(c) and 1(d) we show the opposite situation, here  $\gamma > 0$  and magnetic order is depressed by the appearance of chemical order in the alloy. It is interesting to note that in the completely ferromagnetic case, Fig. 1(d), the temperature difference between  $T_{mo}$  and  $T_{md}$  is always greater than in the ferromagnetic-antiferromagnetic alloy of Fig. 1(c). Also note that since Eqs. (5) and (6) are invariant with respect to either a change of sign of  $K_{AB}$  or a change of sign of both  $K_{AA}$  and  $K_{BB}$ , Fig. 1 shows all

the possible combinations of ferromagnetic and or anti-ferromagnetic couplings.

### III. MAGNETIC TRANSITIONS AT ANTIPHASE BOUNDARIES

Antiphase boundaries form in all ordering alloys. These interesting features of the microstructure of alloys may be observed by transmission electron microscopy and are formed when the rapid growth of the ordered phase from different nucleating centers results in a domain boundary where layers rich in one component are out of register.<sup>1,2</sup> Here we study the composition inhomogeneity induced by the antiphase boundary and its effects on the magnetic properties of the alloy. In particular we examine the planar (001) antiphase boundary in the bcc lattice binary alloy below its ordering temperature  $T_o$ . In this lattice, first-nearest-neighbor sites lie only on consecutive nearest-neighbor planes. Assuming equal occupancies of  $A$  or  $B$  atoms within a given plane, the grand potential  $\omega$  per number of sites in a plane is

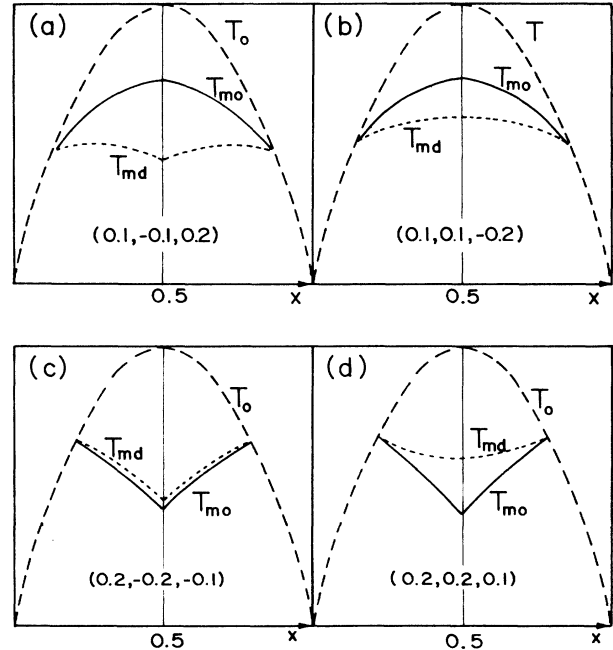


FIG. 1. Magnetic transition temperature for ordered and disordered alloys vs composition. Number in parentheses are values of the interaction parameters  $J_{AA}$ ,  $J_{BB}$ , and  $J_{AB}$ , respectively, in units of the heat of mixing  $\Lambda$ . See text for discussion.

$$\begin{aligned}
\omega = & \frac{k_B T}{2} \sum_i [(1+\xi_i) \ln(1+\xi_i) + (1-\xi_i) \ln(1-\xi_i)] \\
& + \sum_i \left[ \frac{Z\Lambda}{8} \xi_i \xi_{i+1} - \frac{\mu^*}{4} \xi_i \right] + \frac{k_B T}{4} \sum_i (1+\xi_i) [(1+\zeta_i) \ln(1+\zeta_i) + (1-\zeta_i) \ln(1-\zeta_i)] \\
& + \frac{k_B T}{4} \sum_i (1-\xi_i) [(1+\eta_i) \ln(1+\eta_i) + (1-\eta_i) \ln(1-\eta_i)] \\
& + \frac{Z}{8} \sum_i K_{AA} (1+\xi_i) (1+\xi_{i+1}) \zeta_i \zeta_{i+1} + K_{BB} (1-\xi_i) (1-\xi_{i+1}) \eta_i \eta_{i+1} \\
& + K_{AB} [(1+\xi_i) (1-\xi_{i+1}) \zeta_i \eta_{i+1} + (1-\xi_i) (1+\xi_{i+1}) \zeta_{i+1} \eta_i], \tag{9}
\end{aligned}$$

where the index  $i$  runs over all lattice (001) planes. The equilibrium profiles for the occupancies,  $n_{Ai} = 1 - n_{Bi} = (1 + \xi_i)/2$ , and for the magnetization,  $m_i = [S_A(1 + \xi_i)\zeta_i + S_B(1 - \xi_i)\eta_i]/2$  are obtained by minimization of  $\omega$  with respect to  $\xi_i$ ,  $\zeta_i$ , and  $\eta_i$ . An antiphase boundary is built into the system simply by choosing an odd number of planes  $i$  in a closed torus. We obtain the equilibrium profiles through an iterative method with lattices consisting of a total number of sites large enough so that the bulk properties, at a given  $T$  and  $x$ , are reproduced in a considerable region of the torus. Two different profiles may be stabilized in the iterative process, and that in which the majority species accumulates at the APB turns out to be always the most stable.<sup>11</sup>

#### A. $T < T_{mo}$

As mentioned in the preceding section, the onset of magnetic order in alloys may be suppressed by the presence of chemical ordering into sublattices. The disorder introduced by an antiphase boundary then favors the magnetization of the defect in all cases for which  $T_{mo} < T_{md}$ . In Fig. 2 we show the occupancy,  $n_{Ai}$ , and the magnetization,  $m_i$ , profiles associated to the APB for two different sets of magnetic coupling constants. In Fig. 2(a) we show the structure obtained when both pure components are antiferromagnetic but the like-pair coupling is ferromagnetic ( $J_{AA} = -0.2$ ,  $J_{BB} = -0.2$ , and  $J_{AB} = 0.5$ ). The temperature chosen is sufficiently low so that chemical order is almost perfect. Occupancies of species  $A$  are nearly unity in one sublattice and nearly zero in the other for a fixed concentration  $x = \frac{1}{2}$ . The bulk material is ferrimagnetic, however, the enhancement of the magnetization at the interfacial region, together with the signs of the magnetic couplings, result in an antiferromagnetic interaction between the two domains. The net magnetization of the sample vanishes. In the second example one pure species is ferromagnetic and the other antiferromagnetic,  $J_{AA} = -0.2$ ,  $J_{BB} = 0.2$ , and  $J_{AB} = 0.05$ . In Fig. 2(b) we show the profiles for this kind of alloy when it is majority in the ferromagnetic species ( $x = 0.48$ ). The APB results rich also in this component, and the magnetization profile couples the two domains parallel to each other. There is a net mag-

netization in this ferrimagnetic alloy which originates from the APB region. In this system, changes in concentration induce a first-order transition to a state of zero net magnetization, and because  $J_{AA} = -J_{BB}$  this occurs at  $x = 0.5$ , a composition for which two different magnetization profiles coexist. These profiles correspond to parallel and to antiparallel spins near the APB. At higher concentration ( $x = 0.52$ ), as shown in Fig. 2(c) the equilibrium profiles produce no net magnetization and the two domains become coupled antiparallel to each other.

An interesting feature which appears in the regime of parallel alignment of spins at the APB is that the magnetization produced by the defect may point in a direction opposite to the net magnetization of the bulk of the material. In the antisymmetric example described above this may be achieved only if we assign unequal magnetic moments for the two species (say  $S_A > S_B$ ). In Fig. 3 we

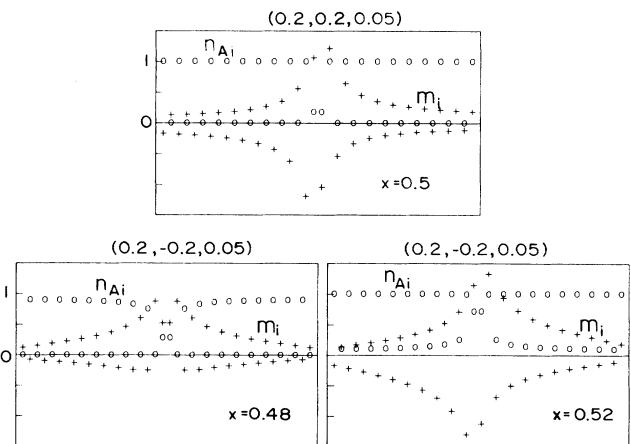


FIG. 2. Magnetization (+) and composition (o) profiles near and APB below the critical magnetization temperature of the bulk ordered alloy. Magnetization is always enhanced at the APB when  $T_{mo} < T_{md}$ , but the coupling between the two domains may be ferromagnetic or antiferromagnetic, numbers in parentheses are the values of the interaction parameters  $J_{AA}$ ,  $J_{BB}$ , and  $J_{AB}$ . See text for details.

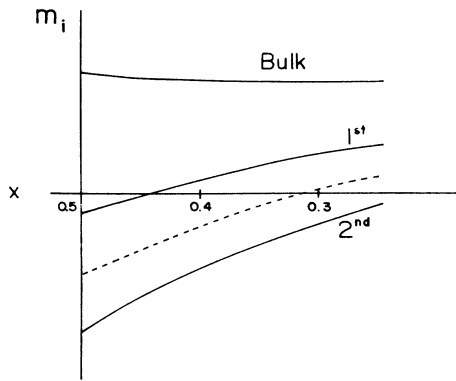


FIG. 3. Layer magnetization for the two layers closest to the center of the APB vs bulk composition for alloys rich in the ferromagnetic species. The temperature is fixed below the ordered alloy magnetization temperatures. The dashed line is the average over the first two layers.

plot the magnetization at the two layers closest to the center of the APB as a function of composition at a fixed temperature  $T < T_{mo}$ . The average over these first two layers is also shown. Within a composition interval ( $0.5 > x > 0.29$ , in our example) the bulk magnetization is reversed with respect to that close to the APB. On the other hand, at low concentrations ( $x < 0.29$ ) there are not sufficient antiferromagnetic components in the system to sustain opposite magnetizations.

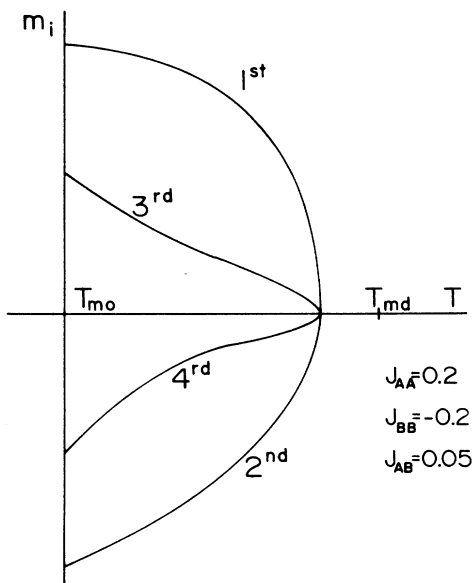


FIG. 4. Magnetization at different layers from the center of the APB for temperatures  $T$  above the bulk magnetic ordered alloy critical temperature  $T_{mo}$ . The magnetic interaction parameters are given in units of the heat of mixing  $\Lambda$ . The composition of the alloy is  $x = 0.5$ .

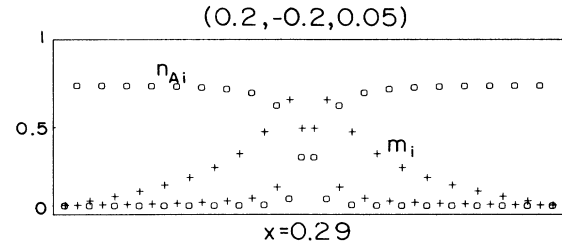


FIG. 5. Magnetization (+) and composition (o) profiles for the APB of the antisymmetric example ( $J_{AA} = -J_{BB}$ ) for a temperature above the bulk critical magnetization temperature of the ordered alloy.

### B. $T > T_{mo}$

Whenever  $T_{mo} < T_{md}$  we find that the magnetization associated to the APB persists at temperatures above the bulk transition temperature  $T_{mo}$  and that a pure interfacial transition occurs at  $T_c^{APB}$ , with  $T_{md} > T_c^{APB} > T_{mo}$ , there the magnetization profile vanishes everywhere. The critical exponent with which the APB magnetization vanishes is that corresponding to a two-dimensional system,<sup>6</sup> however within the mean-field approximation we employ this exponent takes the classical value. In Fig. 4 we show the temperature dependence of  $m$  for four different layers close to the center of the APB for the temperature interval  $T_{mo} < T < T_c^{APB}$  when  $J_{AA} = -0.2$ ,  $J_{BB} = 0.2$ , and  $J_{AB} = 0.05$ .

Thus, at vanishing applied field, a sample consisting of a multidomain structure separated through APB's exhibits within  $T_{mo} < T < T_c^{APB}$  a net magnetization if the majority species couples spins parallel to each other. Lowering the temperature, but still keeping it above  $T_{mo}$ , produces an increment in the width of the magnetized strips along the APB's. This is as if a magnetic phase with critical temperature  $T_c^{APB}$  grows always with the APB's acting as the "nuclei." In Fig. 5 we show composition and magnetization profiles for the antisymmetric example  $J_{AA} = -J_{BB}$  when the majority component is the ferromagnetic species. We observed two magnetic domains pinned to the APB and coupled ferromagnetically which result in a net magnetization of the sample. When a weak external magnetic field is applied to these alloys, lowering the temperature below  $T_{mo}$  may result in a sample with net magnetization with direction opposed to that of the field. The opposite process, i.e., raising the temperature from  $T < T_{mo}$  to  $T_{mo} < T < T_c^{APB}$  also produces a self-reversal which leaves the APB magnetized against the field. The occurrence of this phenomenon is restricted to a range of compositions, as shown in Fig. 3.

## IV. ILMENITE-HAEMATITE SOLID SOLUTION SERIES

In relation to the APB behavior studied in the preceding section we describe briefly some magnetic properties of titanohaematites.<sup>3-5</sup> Natural remanent magnetization of terrestrial rocks corresponds to that acquired in the

geomagnetic field. Minerals containing titanohaematite make an exception and often acquire a remanent moment opposed to the field. Synthesized samples of ilmenite-haematite with compositions near the center of the solid-solution series can show a reverse thermoremanent magnetization which results when a sample is cooled from above its Curie temperature.  $\text{Ilm}_x\text{Hem}_{1-x}$  solutions undergo an ordering transition over the cations at 1100°C for  $x = 65$  and at 600°C for  $x = 45$ , and their ferrimagnetic Curie temperature is sensitive to the thermal history of the sample. Both end members of the series are antiferromagnetic but specimens with  $1 > x \geq 0.5$  are strongly ferromagnetic, while samples with  $0.5 > x \geq 0$  are again antiferromagnetic.<sup>12</sup> Ishikawa and Syono<sup>13</sup> have proposed a mechanism of self-reversal that involves the growth of an  $x$  phase along the boundaries of ordered regions but Hoffman<sup>3</sup> and later Lawson and Nord<sup>4,5</sup> identified the  $x$  phase as an haematite-enriched region along the APB's. As in our model calculations, low concentrations of haematite in the solid solution do not lead to self-reversal, however, a remanent magnetization at  $T > T_{mo}$  (where the specimen is expected to be paramagnetic) is obtained. In many other respects our model calculations agree both with experimental findings and with their current interpretation.

## V. CONCLUSION

Antiphase boundaries are metastable features of the microstructure of ordering alloys, thermal history and treatment may generate or destroy them.<sup>11</sup> The formation of these out of phase ordered domains and their effect on the growth of magnetic domains in magnetic alloys determines magnetic properties of these substances. We have modeled here an interfacial structure for this situation and studied the thermodynamic behavior of the magnetization near the APB's. We found that the critical properties are analogous to those of the surface of a simple Ising ferromagnet with a positive enhancement factor  $g$ , and a pure interfacial magnetic transition develops. We believe that besides the titanohaematites other magnetic solution series may show similar properties at their APB's. The universality of this kind of effect may lead one to consider other examples of interfaces, like those found in magnetic alloys in which the Curie temperature lies above the ordering temperature. In general, all that is required to generate the situation studied here is the interplay of two different order parameters in a given material.

Support was provided in part by Consejo Nacional de Ciencia y Tecnología de México.

\*Present address: Instituto de Física, Universidad Nacional Autónoma de México, Apartado Postal 20-364, México 01000, Distrito Federal, Mexico.

<sup>1</sup>See, for example, D. A. Porter, and K. E. Easterling, *Phase Transformations in Metals and Alloys* (Van Nostrand-Reinhold, United Kingdom, 1981), Chap. 9, p. 363.

<sup>2</sup>R. Kikuchi and J. W. Cahn, *Acta Metall.* **27**, 1337 (1979).

<sup>3</sup>K. A. Hoffman, *Geophys. J. R. Astron. Soc.* **41**, 65 (1975).

<sup>4</sup>C. A. Lawson and G. L. Nord, *Science* **213**, 1372 (1981).

<sup>5</sup>C. A. Lawson and G. L. Nord, *Geophys. Res. Lett.* **11**, 197 (1984).

<sup>6</sup>For a recent review see K. Binder, in *Phase Transitions and Critical Phenomena*, edited by C. Domb and J. L. Lebowitz (Academic, New York, 1986), Vol. 8, Chap. 1.

<sup>7</sup>L. E. Klebanoff, S. W. Robey, G. Lin, and D. A. Shirley,

*Phys. Rev. B* **30**, 1048 (1984); L. E. Klebanoff, R. H. Victora, L. N. Falicov, and D. A. Shirley, *Phys. Rev. B* **32**, 1997 (1985).

<sup>8</sup>D. Weller, S. F. Alvarado, W. Gudat, K. Schröder, and M. Campagna, *Phys. Rev. Lett.* **54**, 1555 (1985).

<sup>9</sup>A. Robledo, C. Varea, and E. Martina, *Phys. Rev. B* **32**, 7545 (1985).

<sup>10</sup>Y. Y. Li, *Phys. Rev.* **102**, 1015 (1956).

<sup>11</sup>L. Vicente, C. Varea, and A. Robledo, *Surf. Sci.* **164**, 479 (1985).

<sup>12</sup>Y. Ishikawa and S. Akimoto, *J. Phys. Soc. Jpn.* **12**, 1083 (1957).

<sup>13</sup>Y. Ishikawa and Y. Syono, *J. Phys. Chem. Solids* **24**, 517 (1963).